Moser, G., Paal, S.G. and Smith, I.F.C. "An electric network for evaluating monitoring strategies intended for hydraullic pressurized networks" Advanced Engineering Informatics, 30, 2016, pp 672-686.
- doi:10.1016/j.aei.2016.09.003

An electrical network for evaluating monitoring strategies intended for hydraulic pressurized networks

GAUDENZ MOSER[1], STEPHANIE GERMAN PAAL[1], DIANE JLELATY[2] AND IAN F.C. SMITH[1]

(1) Applied Computing and Mechanics Laboratory (IMAC)

School of Architecture, Civil and Environmental Engineering (ENAC)

Swiss Federal Institute of Technology (EPFL)

Lausanne, Switzerland

(2) Georgia Tech., Atlanta, USA

Ian.Smith@epfl.ch

Abstract: This paper presents a study of similarities between electrical and hydraulic pressurized networks. The primary objective is to examine whether or not it is possible to use electrical laboratory networks measuring voltage to study leak-region detection strategies measuring flow in water-distribution networks. In this paper, the strategy used to compare the networks is error-domain model falsification, a previously developed methodology for data interpretation that combines engineering knowledge with models and data to enhance decision making. Simulation results obtained for a part of the water-supply network from the city of Lausanne are compared with an analogous electric network. The electrical network is simulated using resistors to mimic the pipes. The consequence is that the electrical model is linear. The resistance values are obtained by computing the hydraulic resistance for each pipe, given by the Hazen-Williams equation. The compatibility of the two networks is evaluated through simulations in three ways: (1) comparing flow predictions obtained by simulating several leak scenarios; (2) comparing the expected identifiability (performance) of the two networks; and (3) comparing sensor placement configurations. The analyses show that even though the models have varying characteristics of underlying physical principles (the electrical model is linear while the hydraulic model is non-linear), the results are within generally accepted engineering limits of similarity (10%). This indicates that measurements on electrical laboratory networks have the potential to illustrate the efficiency and adaptability of leak-detection methodologies for full-scale water-supply and other pressurized hydraulic networks. Finally, two electrical laboratory physical networks, including

an electrical model of part of the water network in Lausanne, were constructed and used in case studies to illustrate this adaptability.

Key words: Water supply network; Leak detection; Model falsification; Sensor placement; Electrical laboratory network

1 Introduction

Fresh water is a key resource in sustainable development. Clean water needs to be preserved and this includes waste prevention. The annual cost of the World's fresh water supply has been estimated to be 184 billion USD [1]. Approximately 5% of this cost (9.6 billion USD) is the consequence of leakage. This represents an average of 20% of clean water supply. These numbers show that there is a need to improve management of fresh-water supply networks. While efficient monitoring systems for leak detection can enhance knowledge, such systems also require advanced sensor-based diagnostic methodologies in order to realize their potential.

Leak detection techniques are usually indirect since measured quantities are used to indirectly infer water loss. Techniques include noise monitoring, pressure monitoring and flow monitoring [2]. The principle of noise monitoring is to capture the noise signal caused by the water flowing through a leak. Other techniques involve measuring variations in the hydraulic state (pressure and flow) due to the presence of a leak. This category can be separated into two groups. The first is transient-based; these techniques use measured transient signals (usually the pressure) to detect leaks [3-7].

The second group is based on the study of steady-state regimes. These techniques can be based on comparisons of measurement with predictions obtained by simulating hydraulic numeric models. Finding predictions corresponding to measurements can be formulated as optimization tasks [8, 9] and by Bayesian inference [10-13]. Weaknesses of these kinds of data-interpretation approaches has been identified by Goulet and Smith [14] and later by Pasquier and Smith [15]. They have shown that approaches such as Bayesian inference and least-square regression may lead to biased identification and prediction with the presence of systematic uncertainties and subsequent unknown correlations, particularly when extrapolating.

Another strategy that can be used to interpret measurement data is model falsification. This principle was first applied to leaks by Robert-Nicoud et al. [16]. Model falsification was developed further by Goulet and Smith [17]; they developed a methodology called error-domain model falsification for infrastructure diagnosis. This methodology was applied to leak-region detection in a preliminary study by Goulet et al. [18] and another study extended this to specific sensor locations [19, 20]. Model falsification typically results in sets of candidate-leak locations that form one or more candidate regions for subsequent investigation using techniques such as acoustic emission.

A challenge associated with developing leak-detection methodologies is that water-distribution networks are difficult to access as they are generally underground. Therefore, monitoring such systems is usually expensive, and once the sensors are installed, moving them to test other sensor configurations is often not feasible. For these reasons, development of a laboratory network is an attractive strategy. However, building hydraulic laboratory networks is costly and working with a network that is complex enough to represent a real network would be arduous. No previous research has been found to address this challenge in combination with an explicit representation of several sources of measurement and modelling uncertainties.

This paper describes a proposal for electrical resistance networks, measuring voltage, that have behavior characteristics which are similar to water distribution networks, measuring flow, and are less complex to build. The paper is a greatly extended version of a previously published conference paper [21]. Through presenting a more extensive range of results, this study goes into much further detail regarding the usefulness of an electrical analogy for water-supply networks. Furthermore, several leak intensities, leak locations and sensor configurations are evaluated for two electrical case studies.

Electrical parallels have already been used by several researchers. Techniques to reduce water distribution networks into a simpler equivalent network have been developed [22, 23]. Oh et al.

[24] reviewed the application of electrical circuits for the analysis of pressure-driven microfluidic networks. Aumeerally and Sitte [25] used electrical networks to model the flow-rate of micro-channels. However, no work has investigated the range of validity of this analogy in the presence of uncertainty.

Electrical analogies have also been used in fields other than hydraulics. Various systems have been modeled by electrical networks such as DNA structures [26-28], stomata networks [29] and tidal stream power resources [30]. However, no previous research has employed electrical networks to test monitoring strategies, such as leak-detection methodologies in water-supply networks.

This paper compares the behavior of a direct current (DC) electrical network model with a hydraulic network model used for leak-region detection using the error-domain model falsification approach for data interpretation. First, the range of validity of this analogy is evaluated in Section 2. Direct similarities are shown by comparing results obtained from simulations of both models. These models are then used to demonstrate similarities through data interpretation in Section 3. Then, two case studies are presented in Section 4 to illustrate the advantage of constructing electrical laboratory networks (Fig. 1). Ultimately it is shown that electrical networks are viable for use as physical surrogates for hydraulic pressurized networks when designing monitoring strategies.

Fig. 1. Flowchart of this study of the electrical-hydraulic analogy. Relevant sections and figures in this paper are noted on the left.

2 Methodology

In Fig. 1, an outline of this study is presented. The purpose of the study is to show similarities between the behavior of hydraulic and electrical network models and to test and evaluate the diagnostic methodology presented in this paper with electrical case studies. In this section, the analogy between electrical and hydraulic networks is presented. This analogy is then used to build a model of an electrical network based on the model of a hydraulic network. Following this, the principle of model falsification as it is applied to leak-region detection is described.

2.1 Hydraulic/electrical analogy

Fig. 2 illustrates the analogy comparing flow in a pressurized pipe with direct current (DC) through a resistor. The Hazen-Williams relation (left) is an empirical relation:

$$\Delta H = 10.674 C^{-1.852} d^{-4.871} L Q^{1.852} = R_{Hydraulic} Q^{1.852} \quad (1)$$

where

ΔH = head loss

Q = flow

d = diameter

L = length

C = Hazen-Williams roughness coefficient C

$R_{Hydraulic}$ = equivalent hydraulic resistance.

While other approximations are available, this formula is typically used by the majority of commercial software in this field (for example, EPANET).

In the electrical case (right), Ohm's law states that:

$$\Delta U = RI \quad (2)$$

where

ΔU = the difference of potential

I = current

R = resistance.

All physical parameters in the Hazen-Williams relation can be combined to form an equivalent hydraulic resistance ($R_{hydraulic}$). This reveals the resemblance between the Hazen-Williams relation and Ohm's law; the difference is that Ohm's law (Eq. 2) is a linear relation while the Hazen-Williams equation (Eq. 1) represents a non-linear relationship (due to the power of the flow, Q).

Fig. 2. Analogy between flow and head loss and hydraulic resistance in a hydraulic pipe and current, potential drop and resistance in an electrical resistor.

In the two curves in Fig. 3, the evolution of flow obtained using Hazen-Williams equation when varying the diameter (a) and head loss (b) and keeping all other variables constant is shown. This illustrates the non-linearity of the Hazen-Williams relation. However, as long as the minimum and maximum diameter and head loss experienced by the network is within a specific range, the relationship can be approximated to be linear. This means that similarities can be expected between electrical and hydraulic models within a specific range. On these curves, the values specific to the city of Lausanne network studied in this paper are noted (100 and 300 mm for the minimum and maximum diameter and 0.05 and 0.45 m for the minimum and

maximum head loss). Differences are generally less than 10% which is a level that is acceptable for engineering purposes, especially considering the high level of uncertainties, see Section 2.2. A linear approximation for such cases can thus be considered appropriate. A more specific requirement is that leak locations are within the set of candidate leak scenarios that describe the leak region. This is described in more detail in Section 2.2.

In this paper, a laboratory model of a DC electrical network with the same general topology as the water supply network for the City of Lausanne is built (Fig.4). Each pipe in the water network is replaced by a resistor in the electrical network. The value of the electrical resistance is obtained by computing the hydraulic resistance of the corresponding pipe using the Hazen-Williams equation.

(a) (b)

Fig. 3. Flow calculated using Hazen-Williams equation with varying pipe diameter (a) and head loss (b).

Each node of the electrical model is connected to a current sink that removes the appropriate amount of current from the network. The tank is the only input of the network. It is modelled using a constant voltage source. In order to compare the results, values of current loss by way of current sinks are calculated to correspond to the value of the demand for the hydraulic network model. In this paper, the networks do not need to be equipped with back flow control devices that force the flow in any one direction. While this kind of element has not been modelled in this study, such an element could be modeled in an electrical network through use of a diode. This study is limited to flow directions that do not reverse.

Fig. 4. Electric-network based on part of the water-distribution network of Lausanne.

2.2 Model falsification

As described in the Introduction, the methodology of model falsification has been presented in refs [16-20] and is summarized in Fig. 5. First, measurements are compared with predictions obtained by simulating several scenarios. Each scenario represents a possible state of the system. A population of scenarios that covers possible behaviors of the system is obtained through combining discrete parameter values describing the identification target. Then, the scenarios that are not compatible with the measurements are eliminated using thresholds determined by a combination of observation and engineering experience. These are called falsified scenarios. Finally, the remaining scenarios, called candidate scenarios, represent system states that explain the measurements within the context of the uncertainties.

Fig. 5. Schema of the falsification process.

This methodology is applied to leak-region detection in water distribution networks. In this case, each scenario corresponds to a set of parameter values that represent characteristics of a leak (location and intensity) and characteristics of the network, such as the level in the tank and the flow entering at the pump. Because a principal parameter of each scenario is the leak, they are called leak scenarios. Leak scenarios are then simulated to obtain predictions of the behavior of the network. Scenario predictions are obtained using steady-state simulations. The assumption is made that the leaks are located at nodes. While this assumption is not always realistic, it is not necessary to add the complexity of leaks occurring at intermediate points of pipes since the data-interpretation goal is to identify leak regions as described in the Introduction.

Another assumption is that there is only one leak occurring at a time. If this methodology is used for continuous monitoring, the hypothesis can be made that two leaks will not appear simultaneously.

Fig. 5 illustrates the error domain model falsification methodology. Measurements (***y***) are compared with predictions (***g(s)***) obtained by simulating each scenario (***s***) with the model (***g()***). In order to compare the measurements and predictions, modelling and measurement uncertainties (u_{model}, u_{meas}) need to be included, such that:

$$\boldsymbol{g}(s) + \boldsymbol{u}_{model} = \boldsymbol{y} + \boldsymbol{u}_{meas} \quad (3)$$

where ***g(s)*** = predictions; ***y*** = measurements; *s* = scenario; $\boldsymbol{u}_{model}$ = modelling uncertainty; and $\boldsymbol{u}_{meas}$ = measurement uncertainty.

More precisely, for each scenario, the values of measurements are subtracted from the values of predictions:

$$\boldsymbol{g}(s) - \boldsymbol{y} = \boldsymbol{u}_{meas} - \boldsymbol{u}_{model} \quad (4)$$

where ***g(s)*** = predictions; ***y*** = measurements; *s* = scenarios $\boldsymbol{u}_{model}$ = modelling uncertainty; and $\boldsymbol{u}_{meas}$ = measurement uncertainty.

Thresholds ($\boldsymbol{T}_{low}$, $\boldsymbol{T}_{high}$) are obtained by combining modelling and measurement uncertainty distributions ($\boldsymbol{u}_{model}$, $\boldsymbol{u}_{meas}$) through Monte Carlo simulations. These distributions are determined from the uncertainty sources described in Section 2.2.1. They are computed at each measurement location by determining 95% bounds of the combined probability function.

If the difference between the measurement and model prediction (i.e., the residual) is not inside the interval defined by the threshold bounds ($\boldsymbol{T}_{low}$, $\boldsymbol{T}_{high}$), the scenario is falsified. The scenarios that remain after the procedure, the candidate scenarios, are those that could explain the measurement values at all measurement locations. Thus, they are calculated such that:

220 $$\boldsymbol{T_{low} \leq g(s) - y \leq T_{high}} \quad (5)$$

221 where $\boldsymbol{g(s)}$ = predictions; $\boldsymbol{y}$ = measurements; s = scenario; and $\boldsymbol{[T_{low}, T_{high}]}$ = lower and upper
222 bound thresholds.

223

224 In Fig. 5, a one-sensor example has been presented. For more sensors, the threshold bounds
225 are obtained with a multi-dimensional pdf using the Šidák correction (see [14]) and an AND
226 condition has to be satisfied –residuals at all sensor locations have to be within the threshold
227 bounds in order for given leak scenario to be a candidate leak scenario.

228 Defining these thresholds is a knowledge intensive task. Evaluating uncertainty values requires
229 extensive engineering experience and knowledge of each uncertainty source (model parameter,
230 model simplifications and measurement uncertainty). The probability of detection of a leak is
231 dependent on the estimation of the uncertainties. The uncertainties are combined to obtain a
232 combined probability distribution function (pdf). The thresholds are fixed on this pdf such that
233 there is a probability of 95% to accept and a 5% probability to reject the correct solution.

234 Measurement uncertainties are due to the sensor resolution and sensor accuracy. Modelling
235 uncertainties include those due to model simplifications and parameter uncertainties. Model
236 simplifications are the consequence of inevitable hypotheses made during development of the
237 mathematical model. For example, in the electrical network model used for this paper, resistors
238 are are assumed to operate without heat dissipation. Such a simplification is common in
239 electronics since the energy lost through heat dissipation often has a negligible effect on
240 performance. Parameter uncertainties are due to errors in the parameter values.

241 For the first part of this study, to enable comparison of the results, the same model and
242 measurement uncertainties have been chosen for both the electrical and hydraulic networks. In
243 reality, these uncertainties are smaller for the electrical network. Measuring current in an

electrical network is more precise than measuring flow in a hydraulic network, and the error associated with Ohm's law is smaller than associated with the Hazen-Williams relation. For the sensor resolution (measurement uncertainties), a uniform distribution with upper and lower bounds at ±2% is used. This value is the tolerance given by the constructor of the flowmeters. For the purpose of comparison, this uncertainty is used in both networks.

For uncertainty due to model simplifications, the assumption is made that the hypotheses used in the mathematical model leads to a *systematic overestimation* of the flow. Various factors could be the source of this overestimation, such as friction and turbulence that occur at bends and fittings. For this study, this simplification uncertainty is thus estimated to be between -30% and 5%. The negative bias in this uncertainty is intended to compensate for the overestimation following Equation (3). Due to a lack of more precise information, an extended uniform distribution [31] was assumed between these two bounds.

For the hydraulic model, the principal parameters that are uncertain are pipe diameter, pipe roughness, minor head loss coefficient, node elevation and nodal demand. Frictional losses dues to roughness and at nodes contribute the most to modelling uncertainty. For the electrical model the parameters are resistance value and nodal demand. However, for this study case, only the nodal demand is considered. The influence of the other parameters on the simulation results is less than 3% when compared with the nodal demand, and therefore, they are neglected. The influence of the demand is so high that it overcomes the other contributions to the uncertainty. The distribution of the nodal demand can completely alter the behaviour of the network whereas the other parameters have a much smaller impact on the output value of the simulation.

The demand at each node (nodal demand) is typically unknown; only the demand of the entire network (global demand) is known. For the two networks, the nodal demand is modelled using an exponential distribution with the mean of the distribution that is equal to global demand

divided by the number of nodes. The global nodal demand used is 0.00694 (cubic meters per second for the hydraulic network and the same quantity of Amperes for the electrical network).

2.3 Expected identifiability

Expected identifiability is a metric used repeatedly for analysis of the results in this paper. Goulet and Smith [32] first developed the metric to predict the number of candidate models that should be obtained using real measurements. Identifiability is described as a criterion which defines the performance of the identification procedure [32]. In this case, expected identifiability is computed by creating simulated measurements. The process is illustrated in Fig. 6.

Fig. 6. Flowchart for defining the expected identifiability metric.

Simulated measurements ($\boldsymbol{y}_s$) are obtained by randomly taking a model instance ($\boldsymbol{g}(s_i)$) in the initial model set and combining uncertainties (($\boldsymbol{u}_{model} - \boldsymbol{u}_{meas}$)) to the predictions:

$$\boldsymbol{y}_s = \boldsymbol{g}(s_i) + (\boldsymbol{u}_{model} - \boldsymbol{u}_{meas}) \quad (6)$$

where $\boldsymbol{y}_s$= simulated measurement; $\boldsymbol{g}(s_i)$ = random model instance; $\boldsymbol{u}_{model}$ = modelling error; and $\boldsymbol{u}_{meas}$ = measurement error.

Many (500) simulated measurements are tested through error-domain model falsification in the same way as represented in Equations (3-5):

$$\boldsymbol{T_{low}} \leq \boldsymbol{g}(s) - \boldsymbol{y}_s \leq \boldsymbol{T_{high}} \quad (7)$$

where $\boldsymbol{y}_s$= simulated measurement; $\boldsymbol{g}(s)$ = random model instance; and [$\boldsymbol{T_{low}}$,$\boldsymbol{T_{high}}$] = lower and upper bound thresholds.

For each measurement, the number of candidate models is computed and saved. Results are used to build a cumulative distribution function (CDF) that represents the probabilities to obtain a number of candidate models less than or equal to a specific number (definition of a cumulative distribution function). This CDF is the expected identifiability [32]. It represents the capacity of the system to identify leaks. More specifically, for this work, this CDF is built by testing a large number of simulated leaks on the network. For each leak, the number of candidate scenarios is computed using error-domain model falsification (Eq. 6, 7). Then the cumulative distribution is computed.

This measure indicates the performance of the diagnosis for a given sensor configuration. For example, this metric indicates the maximum number of candidate models that are expected for a given probability. A lower number of candidate models for a given probability indicates a better diagnostic performance than a higher number of candidate models. The ideal performance is to have a 100% probability to obtain one candidate model that is able to explain the measurements at a 95% reliability of identification. In this case, the system is unambiguously identified.

2.4 Sensor placement

The sensor placement strategy used in this paper was adapted from the one proposed by Goulet and Smith [32]. For each sensor configuration the expected identifiability is computed for a 95% probability, and the sensor configuration selected as the best one is the configuration with the smallest number of expected candidate models. To reduce the number of solutions to test, they associated this strategy with a forward greedy algorithm where the objective function was the expected identifiability.

The first step is to find the best location for one sensor. All potential sensor locations are tested. According to the objective function, the best one is chosen. Once the location for one sensor

has been chosen, the second step is to search all potential locations for the second sensor. The principle of a greedy algorithm is to limit the search domain by considering that the solution found previously for one sensor is part of the solution for two sensors. This reduces the search for the locations of the second sensor. This process is repeated to find the optimal configuration for the desired number of sensors.

The number of combinations tested with a greedy algorithm is N+ (N-1) + (N-2) +…+1. Therefore, using a greedy algorithm reduces the number of combinations to test from 2^N to $N(N+1)/2$. While the solution which is found may not be a global optimum, this algorithm has been found to provide results that are not significantly different from the global optimum in practical cases [18].

3 Hydraulic/electrical comparison

This section compares the behavior of the electric and the hydraulic networks to evaluate whether or not the analogy will suffice for the purposes outlined in this work. First, predictions obtained by simulating leak scenarios are studied in order to directly compare the behavior of the two models. Then, the two models are compared through model falsification by looking at the performance of the identification procedure. Finally, a sensor placement study is carried out to ensure that both models lead to sensor configurations with similar performance. For all of these results, the hydraulic network has been modelled and simulated using the software, Epanet. The software, Simulink, has been used for the electric network.

Fig. 7. Comparison of predicted values obtained by simulating leak scenarios at three sensor locations.

Fig. 7 illustrates a comparison of the flow and current obtained by simulating leak scenarios using the hydraulic and electrical models for three sensor locations. The horizontal axes refer

to the individual leak scenarios. The vertical axes display the flow in cubic meters per second for the hydraulic model and the current in Amperes for the electric model. The sensor values for each scenario are joined by lines in order to increase clarity (though they have no physical meaning).

Differences between the two data-plots are evident when looking directly at the magnitude of the values obtained for each scenario. However, by observing the data together (the shape of the data-plot), the two plots are comparable. Peaks and valleys are obtained for the same leak scenarios. This shows that, although the electric model is linear and the hydraulic model is non-linear, the behavior of the two models is similar. While it is encouraging that the electric and hydraulic models have such similar behavior, the aim of this study is to show similarity throughout the process of model falsification to identify sets of candidate models and, subsequently, critical regions for local inspection. This similarity is studied in the following section.

3.1 Model falsification comparison

The hydraulic and electric models have both been used for leak/loss detection using model falsification (Eq. 5). Fig. 8 shows four examples of leak-region detection in the electrical (left column) and hydraulic (right column) networks. For each example, the same leak (position an intensity (125 l/min or 0.002083 m^3/s flow and 0.002083 A current) is studied through the electrical and hydraulic models. Each leak position is displayed by four arrows. The sensor positions are represented by black squares, the demand nodes are indicated by white circles and the pipes by grey lines. The black dots show positions of candidate leak scenarios. The voltage source and tank is designated on each subfigure for the electrical and hydraulic networks, respectively.

The areas defined by the candidate leak scenarios, termed “leak regions,” are similar for the four examples differing only by a few nodes. This implies that electrical networks can be used to perform leak-region detection for hydraulic networks, regardless of the leak location.

Fig. 8. Comparison of leak-region detection results using simulations of the electrical (left, Eq. 2) and hydraulic (right, Eq. 1) networks for four leak locations.

The analysis of the candidate scenarios obtained for simulation of each of the 94 leak locations shows that, on average, 85 percent of candidate scenarios obtained using the hydraulic model are identical to those obtained using the electric model. For each case, the number of candidate leak scenarios that are found, either with only the electric model or with only the hydraulic model, is calculated. On average there are only seven scenarios that differ when comparing the electric and hydraulic model behaviors through model falsification.

Fig. 9. Comparison of the evolution of expected identifiability (Fig. 6) with simulations of four cases of leak intensity noted in the figure as circled numbers.

In Fig. 9, a comparison of the expected identifiability across varying degrees of leak intensity is displayed. The probability is displayed on the vertical axis, and the number of expected candidate scenarios is shown on the horizontal axis. The black curves represent the electrical model while the hydraulic model results are marked by grey curves. The leak intensities for each set of curves are marked on the plot.

The results in Fig. 9 indicate that the leak intensity has little influence on the behavior trends through model falsification, particularly for low numbers of candidate models. In the four cases, the curves follow the same shape, and the decrease in performance from the hydraulic network to the electrical network is generally less than 10% for the same leak intensity. Curves diverge

when the number of candidate models increases beyond approximately 40% of the number of models in the initial model set. Most measurement systems are configured to do better than this. Also, for all four scenarios, the difference is not significant (the difference in performance between both the electrical and hydraulic models does not increase or decrease when the leak intensity changes). This implies that electrical networks can be used for leak-region detection in hydraulic networks for a range of leak intensities.

3.2 Sensor placement comparison

A sensor placement study has been carried out using the hydraulic and electrical models. A greedy algorithm with the objective function set to increase the expected identifiability for a probability of 95% was used [18]. A greedy algorithm sequentially selects the sensor location that best satisfies the objective function without putting into question previous selected positions. At each step of the greedy algorithm, expected identifiability is calculated for all sensor location alternatives for a 95% probability. The solution with the best results (i.e. the highest expected number of falsified models) is selected.

Fig. 10. Comparison of the curve that gives the relation between the expected number of falsified leak scenarios (obtained through simulations with a probability of 95%) (Eq. 5) and the number of measurements used.

In Fig. 10, the comparison of the sensor placement results for the electrical and hydraulic networks is presented. On the vertical axis, the expected number of falsified leak scenarios is represented, and the number of measurement locations is displayed on the horizontal axis. The black points represent the electrical model, while the grey points represent the hydraulic model. Each point represents the expected performance for a number of measurement locations, given the expected number of leak scenarios for a probability of 95%.

Fig. 11. Sensor placement results using simulation with a greedy algorithm for 15 and five sensors.

Fig. 11 illustrates the sensor configurations obtained for two cases: (1) with 15 measurements (top); and (2) with five measurements (bottom). The positions of the measurements are given by black squares for the electrical model and white stars for the hydraulic model. The sensor configurations are not identical. Small differences in performance may have an influence on the sensors chosen in this process. In a greedy sensor placement, the selection of a sensor location at a given step is dependent on the sensor locations obtained at all previous steps in the process. For this reason, if the small differences between the electrical and hydraulic models cause the algorithm to select a different sensor in the first step of the process, then the greedy algorithm can lead to varying solutions. However, the performance of the two sensor configurations remains similar, as described next.

(a) (b)

Fig. 12. Comparison of expected identifiability (Fig. 6) using simulations of the electrical and hydraulic networks with the 15 sensor configuration obtained using the Greedy algorithm for a) the electrical model and b) the hydraulic model.

Fig. 12 illustrates a comparison of the expected identifiability for the hydraulic and electrical networks with a configuration of 15 sensors obtained using the Greedy algorithm with (a) the electrical network and (b) the hydraulic network as a starting point. The vertical axis displays the probability, and the horizontal axis displays the expected number of candidate leak scenarios considering all leak scenarios (50-125 l/min - 376 leak scenarios).

These results show that the performance of the diagnosis using the hydraulic model is adequate even if the sensor configuration is obtained using the electrical network model and vice versa.

Figure 12 shows that the difference of performance, in terms of expected number of candidate models, is small regardless of which network is used for the sensor placement.

All findings indicate that low-cost electrical laboratory networks can be built and used to test sensor placement strategies and leak-region detection performance for a range of water distribution networks. Differences are less than 10%, which is acceptable in engineering contexts.

4 Electrical case studies

In this section, two case studies are presented in order to illustrate the efficacy of using physical (not simulated) electrical networks to represent water-distribution networks and, within the context previous work [16-20], to further demonstrate the potential for using error-domain model falsification for leak-region detection. The goal in the previous section was to compare the behavior of the two simulation models. In order to be able to compare the results, the same uncertainties were used in both cases. Therefore, the uncertainties have been over estimated for the electrical network. In this section, physical electrical networks are employed, and true uncertainty values have been used for the electrical networks. In both case studies, the leak measure used is the difference of potential associated with the resistor.

4.1 City of Lausanne

The first case study is based on a physical electrical network similar to part of the network of the city of Lausanne, see Fig. 4. The network is supplied with a continuous voltage source with potential of 18V. In order to simulate the demand, some nodes were connected through resistors to ground. Leaks are simulated in the same way.

4.1.1 Uncertainty estimation

The uncertainty due to model simplification is estimated by comparing measurements and predictions for each resistor. This was achieved for the undisturbed network (no leaks). Fig. 13 (a) shows the results of a comparison between measurements and predictions for each resistor in a network with no leaks. The vertical axis is the relative error between measurements and predictions and the horizontal axis shows resistors labels. The results indicate that the relative error is between -5% and +5% in all cases. Fig. 13 (b) shows a comparison between laboratory measurements on the physical electrical network and simulation predictions through a histogram. In order to simplify, the uncertainty is taken to be a uniform distribution between -4.5% and +5%. In this plot, a small bias associated with the model simplification uncertainty is revealed. Such a bias is to be expected since there are often many sources of systematic modelling uncertainties due to inevitable modelling assumptions.

The secondary parameters are the uncertainties associated with the resistor values. The resistors of the E96 series that were used have a standard uncertainty of +/- 1%. The measurement uncertainty is thus evaluated as +/- 1%.

(a) (b)

Fig. 13. Relative error between measurements of the physical electrical network and predictions for each sensor.

4.1.2 Sensor placement

Sensor placement was carried out using a greedy algorithm (see Section 2.4), with the optimization objective to maximize the expected identifiability. The sensor placement study was carried out using prior knowledge of the demand in this case. In reality, this is not possible;

477 the sensors have to perform in a range of demand conditions. In hydraulic full-scale cases,
478 sensor placement is determined with a general shape for demand, such as the exponential law.
479 The relationship between the expected numbers of falsified leak scenarios and the number of
480 measurements for the electrical network of the city of Lausanne is shown in Fig. 14.

481

482 **Fig. 14.** Sensor placement curve giving the relation between the expected numbers of falsified leak scenarios
483 (simulations with a probability of 95%) (Eq. 5) and the number of measurements used.

484 The number of measurements used is displayed on the horizontal axis while the expected
485 number of falsified models as a percentage of the total number of models in the initial model
486 set is displayed on the vertical axis. The sensor placement curve shows that, for this case study,
487 the performance increases significantly from one to four sensors.

488 Two sensor configurations are tested in this study: first, a configuration with three sensors, and
489 second, a configuration with six sensors. Fig. 15 shows the performance for a current loss of
490 0.002 mA. The number of candidate leak scenarios is displayed on the horizontal axis while the
491 cumulative probability (the probability that the value of a random variable falls within a
492 specified range) for each sensor configuration is displayed on the vertical axis. The results show
493 that the performance is good in both cases. The expected identifiability shows that the
494 performance is much better when uncertainties are reduced; three sensors perform almost as
495 well as six sensors. These results are based on simulated measurements. An examination of the
496 performance using real measurements is carried out next.

497

498 **Fig. 15.** Expected identifiability (Fig. 6) for simulations of three and six sensor configurations, for a current loss
499 of 0.002 mA.

500 4.1.3 Leak-region detection

501 For this case study, the leak detection (current loss) is carried out at several locations through
502 application of error-domain model falsification. The results are given for the two sensor
503 configurations presented in Section 4.1.2. Fig. 16 shows the leak (current loss) detection results
504 for four leak locations and two sensor configurations (three sensors (left column) and six
505 sensors (right column)). These results are not numerical simulations; real measurements have
506 been carried out in the laboratory on the physical electrical network. Each leak position is
507 displayed by four arrows. The sensor positions are represented by black squares, the demand
508 nodes are represented by white circles and the pipes by grey lines. The black dots show positions
509 of candidate leak scenarios. Ground and voltage source are designated on each subfigure.

510 The results show that when the parameters of the network are controlled and well known, the
511 leak-region detection can be accurate. In addition, a high number of sensor is not necessary. In
512 the first two cases (top two rows), the number of candidate models is reduced to three (first
513 case) and one (second case) using only three sensors. The third and fourth leaks (bottom two
514 rows) illustrate the case where adding more sensors helps to falsify outlier candidates (on the
515 left part of the network) in addition to reducing the size of the leak region.

516

517 **Fig. 16.** Leak-region detection for measurements on physical electrical networks having four leak locations and
518 two sensor configurations for a current loss of 0.002 mA.

519 The results of this case study illustrate that error domain model falsification can be successfully
520 used for leak-region detection when uncertainties are reduced. When the nodal demands are
521 well known, the model is more precise and this results in better predictions.

4.2 10 x 10 square network

The second electrical case study is based on a square network made up of 100 junctions (10x10) and 180 10KΩ resistors (Fig. 17). The network is supplied with a 12 V continuous voltage source shown in the bottom left corner. Three leak locations are studied on this network (marked by four arrows in the figure). The leak is modelled with a variable resistor (potentiometer). For this case study the demand is fixed at zero; there is no output other than the leak. This can be representative of a network in a residential area where the lowest consumption is near zero due to small use of water during the night.

Fig. 17. Illustration of the 10x10 square electrical network.

4.2.1 Uncertainty

The uncertainties are the same as in the laboratory network for the city of Lausanne (described in the previous sections). The uncertainty due to model simplifications is a uniform distribution between -4.5% and +5%. The resolution of the sensors is estimated at +/- 1%, and the uncertainty of the resistance values is estimated at +/- 1%.

4.2.2 Sensor placement

Sensor placement was carried out using a greedy algorithm as described in Section 2.4, with the optimization objective to maximize the expected identifiability and a current loss of 0.3 mA. The relation between the expected numbers of falsified models obtained through simulations (Eq. 5) and the numbers of measurements (Fig. 18) shows the percentage of falsified models for a 95% probability for up to ten sensors. On the horizontal axis the number of measurements (sensors from one to ten) is designated, and on the vertical axis the corresponding expected

number of falsified models is displayed. These results demonstrate that, in the case where the uncertainty related to the demand is nonexistent, the identification performance is sufficient (90%) with just four sensors.

Fig. 18. Sensor placement curve giving the relation between the expected numbers of falsified models obtained through simulations (Eq. 5) and the number of measurements.

Fig. 19. Simulation results revealing the expected number of candidate models as a function of the leak intensity and the number of measurements for a 95% probability (left) and a 75% probability (right).

Fig. 19 shows the expected number of candidate models for a probability of 95% (left) and 75% (right) for three leak intensities (0.1, 0.3, 0.5 mA) and for one to ten measurements. These intensities correspond to real leak intensities of 6, 18 and 30 l/min in a pipe of 120mm diameter that is 155m long having Hazen-Williams roughness coefficient of 100. Results show that the performance of the identification decreases (more candidate models) with decreasing leak intensity. For a leak intensity of 0.3 and 0.5 mA, the performance is good even for a small number of measurements. For a leak intensity of 0.1 mA the performance decreases rapidly from three to one sensors.

This reveals upper bounds of leak-region detection performance for sensor configurations of full-scale water distribution networks. These bounds are important for decision making such as selecting the number and positions of sensors in a network.

4.2.3 Leak-region detection

For this case study, the leak (current loss) detection is achieved for two leak intensities: 0.3 mA and 0.5 mA using error-domain model falsification. These leaks are tested at three different locations on the network. Some of the results are given in Fig. 20. Each leak is represented by

569 the four arrows. Each demand node is designated by a white circle, while the pipes are
570 designated by the black links between the demand nodes. The sensors are designated by black
571 squares, and the candidate leak scenarios are designated by black dots. Ground and voltage
572 source are also designated on each subfigure. The results show that the identification of the leak
573 region improves with the magnitude of the leak intensity since there are lower numbers of
574 candidate leak scenarios.

575 These results can be compared to the expected number of candidate models that have been
576 obtained with simulated measurements. Fig. 21 shows this comparison for leak intensities of
577 0.3 mA (left) and 0.5 mA (right) and for one to ten measurements. The darkest grey bars
578 designate the expected number of candidate models for a probability of 95%. For a leak
579 intensity of 0.5 mA, the number of candidate models is closer to the expected number than for
580 the 0.3 mA leak intensity for the first two leak cases. For the third leak case, with one sensor,
581 the results are worse than the expected values based on simulations. Leak 3 cases of 6, 3 and
582 one measurement(s) with 0.3 mA leak intensity are distant from the expected number of
583 candidate models. Nevertheless, these results indicate that for the majority of leak cases, the
584 experimental results are in line with the simulations.

585 This study illustrates through three leak examples how the identification performance increases
586 when the leak intensity and number of sensors increase. The behavior obtained through
587 experiments confirms the expected identifiability predicted with simulated measurements.

588

589

590 **Fig. 20.** Leak-region detection results for sensor measurements and leaks in the physical 10x10 electrical
591 network.

Fig. 21. Comparison between results obtained with measurements on the physical network and expected identifiability obtained through simulations (Fig. 6).

5 Conclusions

Determination of appropriate analogies of complex systems is dependent upon the data interpretation strategy that is used for performance assessment. In this paper the data-interpretation strategy assumed is error-domain model falsification, a previously-proposed methodology that combines engineering knowledge with models and data to enhance decision making.

Analyses of the results lead to the following conclusions.

Low-cost electrical laboratory networks can be built and used to test sensor placement strategies and leak-region detection performance for a range of water distribution networks, provided that pipe diameters and head losses are within a range where the linear approximation is within 10% of the non-linear behavior.

Electrical networks provide a physical test-bed that is complementary to numerical simulations, thereby allowing engineers to base decisions on combinations of simulations and measurements.

Leak-detection performance may be significantly improved when demand uncertainty is reduced.

Studies of physical electrical resistance networks reveal upper bounds of leak-region detection performance for sensor configurations of full-scale water distribution networks. These bounds are important for decision making such as selecting the number and positions of sensors in a

network. For example, even if it is possible to reduce uncertainties to very low values in a full-scale network, performance will never be better than that reflected by tests on an electrical network.

6 Acknowledgments

This research is part of the Water Resources Innovation Program of EPFL Middle East and is funded by EPFL Middle East. The authors acknowledge the support from Eau Service, the water provider of the city of Lausanne. This journal paper is an extended version of a previously presented conference paper: Moser, G., German Paal, S. & Smith, I.F.C. 2015. Using electrical resistance networks to enhance performance assessments of water distribution networks. 7th International Conference on Structural Health Monitoring of Intelligent Infrastructure (SHMII), Torino, Italy, 2015.

7 References

[1] Sensus, *Water 20/20: Bringing smart water networks into focus.* Technical report, 2012.

[2] Xu, Q., Liu, R., Chen, Q. & Li, R. 2014. Review on water leakage control in distribution networks and the associated environmental benefits. *Journal of Environmental Sciences,* 26**,** 955-961.

[3] Vítkovský, J. P., Simpson, A. R. & Lambert, M. 2000. Leak detection and calibration using transients and genetic algorithms. *Water Resources Planning and Management***,** 258–262.

[4] Vítkovský, J. P., Lambert, M. F., Simpson, A. R. & Liggett, J. A. 2007. Experimental observation and analysis of inverse transients for pipeline leak detection. *Journal of Water Resources Planning and Management,* 133**,** 519.

[5] Whittle, A. J., Girod, L., Preis, A., Allen, M., Lim, H. B., Iqbal, M., Srirangarajan, S., Fu, C., Wong, K. J. & Goldsmith, D. 2010. WATERWISE@ SG: A testbed for continuous monitoring of the water distribution system in singapore. *Water Distribution System Analysis, WSDA.*

[6] Whittle, A., Allen, M., Preis, A. & Iqbal, M. 2013. SENSOR NETWORKS FOR MONITORING AND CONTROL OF WATER DISTRIBUTION SYSTEMS. *Proceedings of The 6th International Conference on Structural Health Monitorinf of Intelligent Infrastructure,* Hong Kong.

[7] Srirangarajan, S., Allen, M., Preis, A., Iqbal, M., Lim, H. B. & Whittle, A. J. 2010. Water main burst event detection and localization. *Proceedings of Proceedings of 12th Water Distribution Systems Analysis Conference (WDSA'10).*

[8] Pudar, R. S. & Liggett, J. A. 1992. Leaks in Pipe Networks. *Journal of Hydraulic Engineering,* 118**,** 1031-1046.

[9] Andersen, J. H. & Powell, R. S. 2000. Implicit state-estimation technique for water network monitoring. *Urban Water,* 2**,** 123-130.

[10] Poulakis, Z., Valougeorgis, D. & Papadimitriou, C. 2003. Leakage detection in water pipe networks using a Bayesian probabilistic framework. *Probabilistic Engineering Mechanics,* 18**,** 315-327.

[11] Rougier, J. 2005. Probabilistic leak detection in pipelines using the mass imbalance approach. *Journal of Hydraulic Research,* 43**,** 556-566.

[12] Puust, R., Kapelan, Z., Koppel, T. & Savic, D. 2006. Probabilistic Leak Detection in Pipe Networks Using the SCEM-UA Algorithm. *Proceedings of Water Distribution Systems Analysis Symposium 2006,* Cincinnati, Ohio, USA. 1-12. ASCE (American Society of Civil Engineers).

[13] Barandouzi, M. A., Mahinthakumar, G., Brill, E. D. & Ranjithan, R. 2012. Probabilistic Mapping of Water Leakage Characterizations Using a Bayesian Approach. *Proceedings of World Environmental and Water Resources Congress 2012*, Albuquerque, New Mexico, USA. 3248-3256. ASCE (American Society of Civil Engineers).

[14] Goulet, J.-A. & Smith, I. F. C. 2013. Structural identification with systematic errors and unknown uncertainty dependencies. *Computers & structures,* 128**,** 251-258.

[15] Pasquier, R. and I.F.C. Smith, *Robust system identification and model predictions in the presence of systematic uncertainty.* Advanced Engineering Informatics, 2015.

[16] Robert-Nicoud, Y., Raphael, B. & Smith, I. 2005. Configuration of measurement systems using Shannon's entropy function. *Computers & structures,* 83**,** 599-612.

[17] Goulet, J.-A. & Smith, I. F. C. 2013. Predicting the Usefulness of Monitoring for Identifying the Behavior of Structures. *Journal of Structural Engineering,* 139**,** 1716-1727.

[18] Goulet, J.-A., Coutu, S. & Smith, I. F. C. 2013. Model falsification diagnosis and sensor placement for leak detection in pressurized pipe networks. *Advanced Engineering Informatics,* 27**,** 261-269.

[19] Moser, G. & Smith, I. F. C. 2013. Detecting leak regions through model falsification. *Proceedings of 20th International Workshop: Intelligent Computing in Engineering 2013*, Vienna, Austria. European Group for Intelligent Computing in Engineering (EG-ICE).

[20] Moser, G., Paal, S. G., & Smith, I. F. (2015). Performance comparison of reduced models for leak detection in water distribution networks. *Advanced Engineering Informatics*, *29*(3), 714-726.

[21] Moser, G., German Paal, S. & Smith, I.F.C. 2015. Using electrical resistance networks to enhance performance assessments of water distribution networks. 7th International Conference on Structural Health Monitoring of Intelligent Infrastructure (SHMII), Torino, Italy, 2015.

[22] Ulanicki, B., Zehnpfund, A. & Martinez, F. 1996. Simplification of water distribution network models. *Proceedings of Second International Conference on Hydroinformatics,* Zürich, Switzerland. 493-500. IAHR (International Association for Hydraulic Research).

[23] Martinez Alzamora, F., Ulanicki, B. & Salomons, E. 2014. Fast and Practical Method for Model Reduction of Large-Scale Water-Distribution Networks. *Journal of Water Resources Planning and Management,* 140**,** 444-456.

[24] Oh, K. W., Lee, K., Ahn, B. & Furlani, E. P. 2012. Design of pressure-driven microfluidic networks using electric circuit analogy. *Lab on a Chip,* 12**,** 515-545.

[25] Aumeerally, M. & Sitte, R. 2006. Layered fluid model and flow simulation for microchannels using electrical networks. *Simulation Modelling Practice and Theory,* 14**,** 82-94.

686 [26] Marshall, R. 2009. Modeling amino acid strings using electrical ladder circuits. *Proceedings of*
687 *Nature & Biologically Inspired Computing, 2009. NaBIC 2009. World Congress on*. 1580-1583.
688 IEEE.

689 [27] Marshall, R. 2010. Modeling DNA/RNA Strings Using Resistor—Capacitor (RC) Ladder
690 Networks. *The Computer Journal*, 53**,** 644-660.

691 [28] Roy, T., Das, S. & Barman, S. 2014. Electrical Network Modeling of Amino Acid String and Its
692 Application in Cancer Cell Prediction. *In:* MOHAPATRA, D. P. & PATNAIK, S. (eds.) *Intelligent*
693 *Computing, Networking, and Informatics.* Chapter 28.

694 [29] Berg, D. 2014. Creating an Electronic Analog of a Stomatal Network. *Physics Capstone Project,*
695 Paper 5.

696 [30] Draper, S., Adcock, T. a. A., Borthwick, A. G. L. & Houlsby, G. T. 2014. An electrical analogy for
697 the Pentland Firth tidal stream power resource. *Proceedings of the Royal Society A: Mathematical,*
698 *Physical and Engineering Science*, 470.

699 [31] Goulet, J.-A. & Smith, I. F. C. 2011. Extended Uniform Distribution Accounting for Uncertainty
700 of Uncertainty. *Vulnerability, Uncertainty, and Risk: Analysis, Modeling, and Management.*
701 Hyattsville, Maryland, United States: ASCE (American Society American Society of Civil
702 Engineers).

703 [32] Goulet, J. and I. Smith, *Performance-Driven Measurement System Design for Structural*
704 *Identification*. Journal of Computing in Civil Engineering, 2012. **27**(4): p. 427-436.

705

706

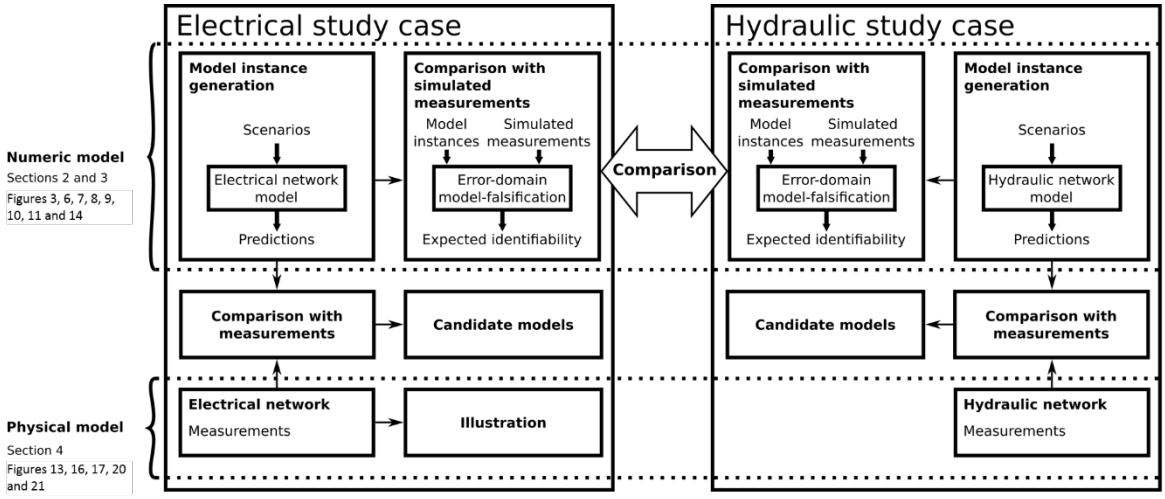

Fig. 1. Flowchart of this study of the electrical-hydraulic analogy. Relevant sections and figures in this paper are noted on the left.

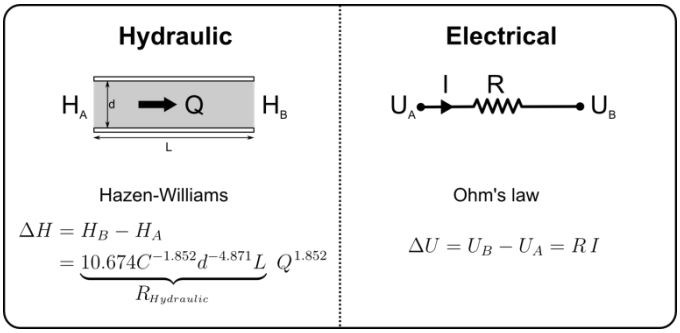

Fig. 2. Analogy between flow and head loss and hydraulic resistance in a hydraulic pipe and current, potential drop and resistance in an electrical resistor.

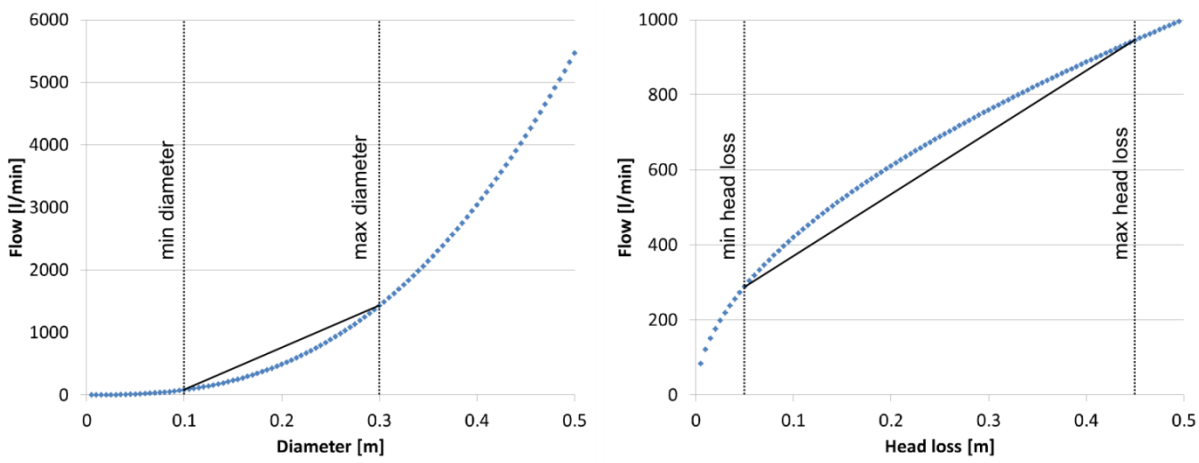

(a) (b)

Fig. 3. Flow calculated using Hazen-Williams equation with varying pipe diameter (a) and head loss (b).

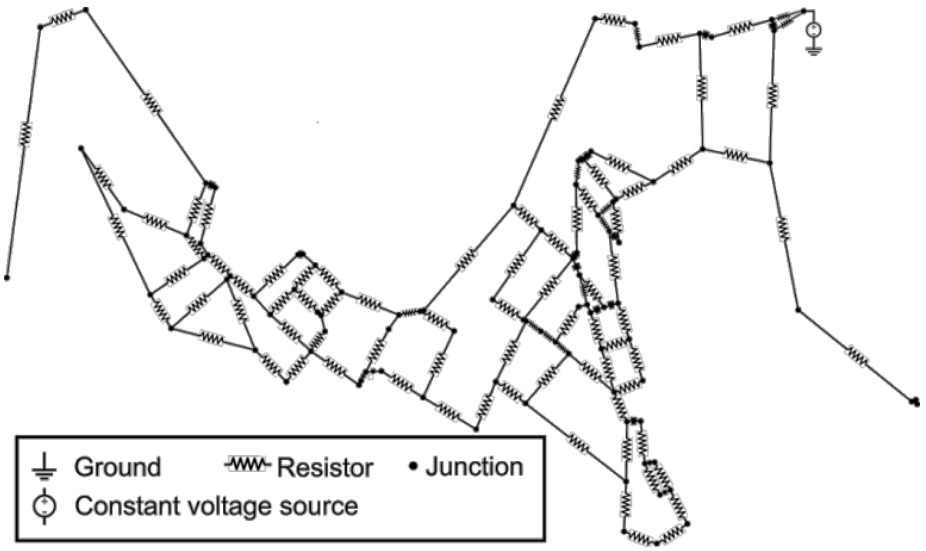

Fig. 4. Electric-network based on part of the water-distribution network of Lausanne.

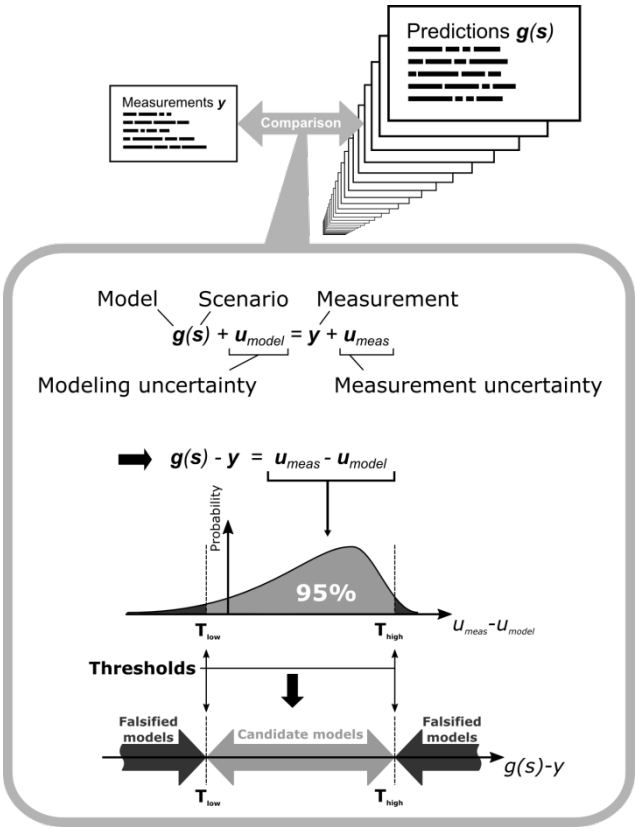

727

728 **Fig. 5.** Schema of the falsification methodology.

729

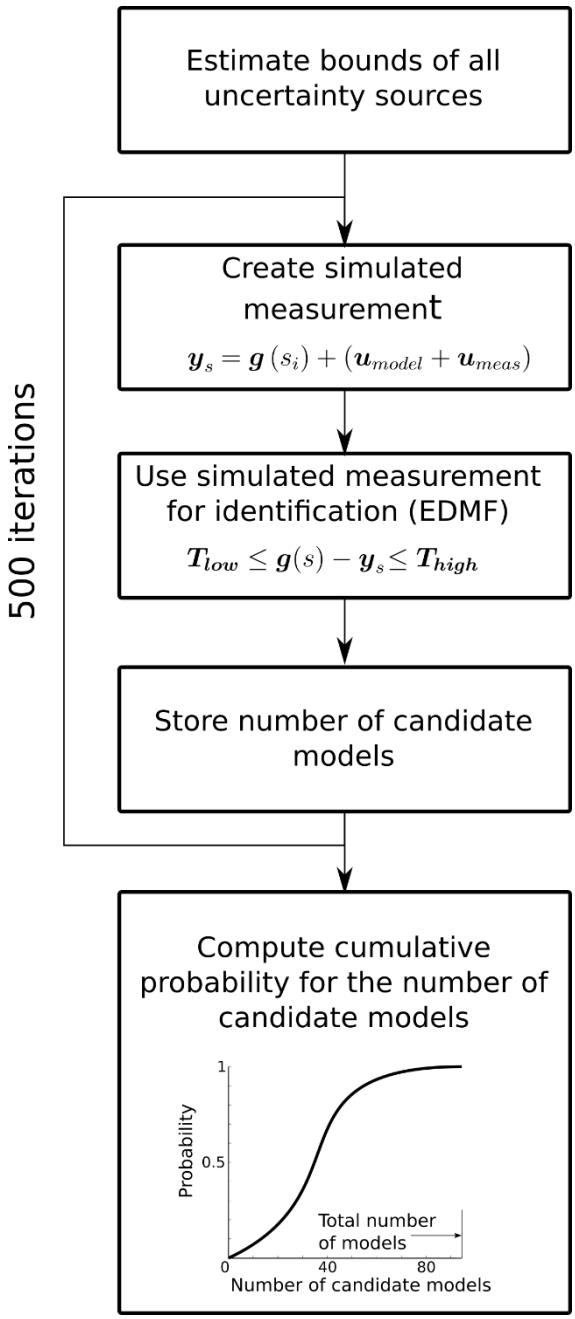

Fig. 6. Flowchart for defining the expected identifiability metric.

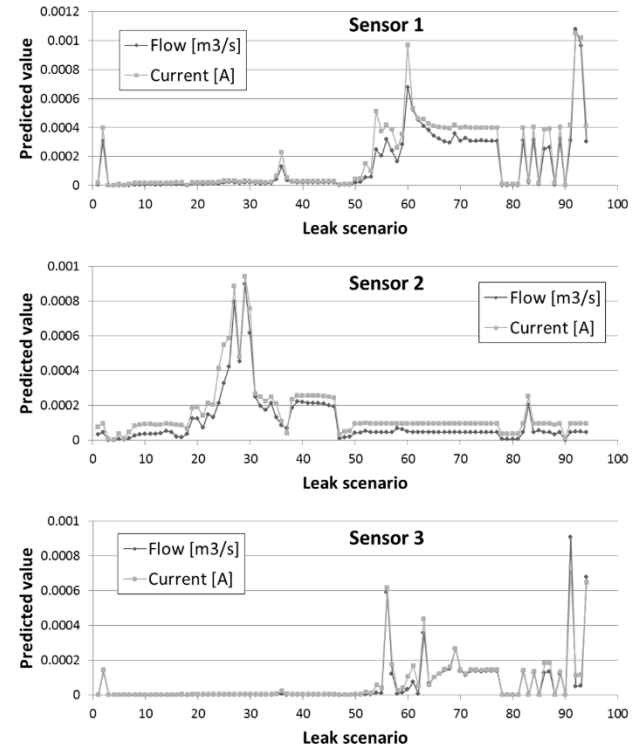

Fig. 7. Comparison of predicted values obtained by simulating leak scenarios at three sensor locations.

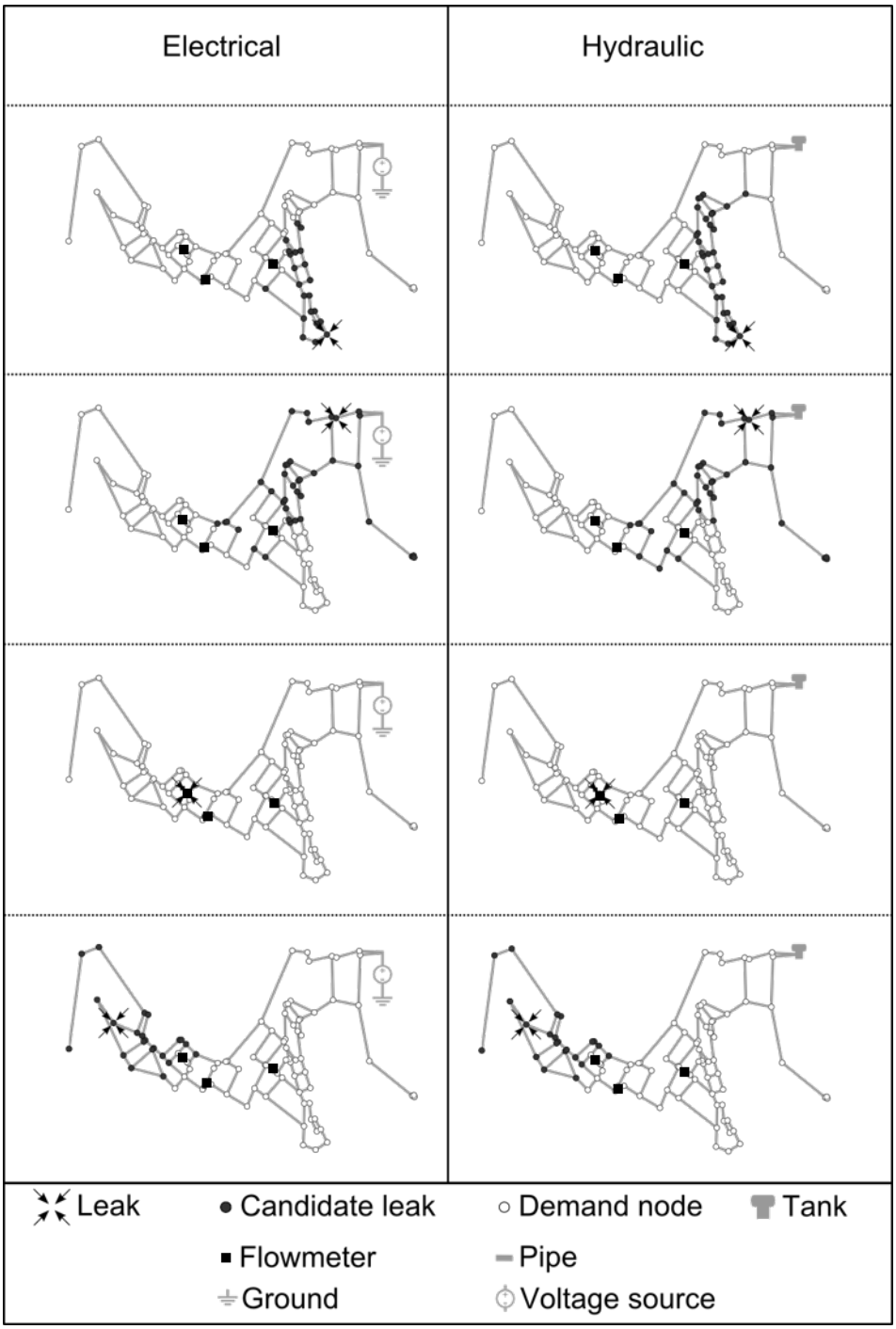

Fig. 8. Comparison of leak-region detection results using simulations of the electrical (left, Eq. 2) and hydraulic (right, Eq. 1) networks for four leak locations.

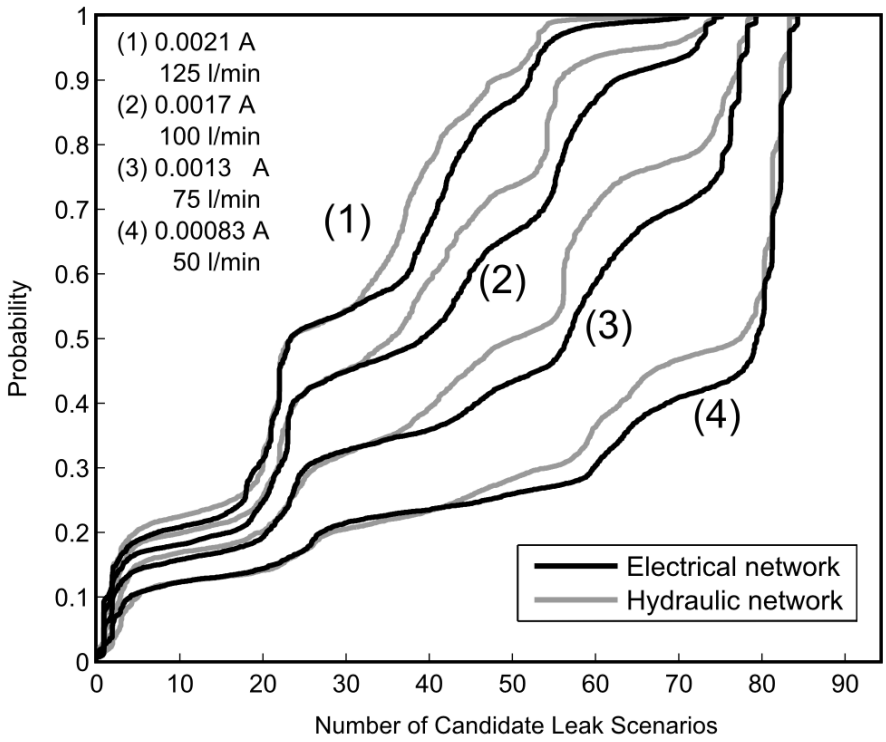

751

752 **Fig. 9.** Comparison of the evolution of expected identifiability (Fig. 6) with simulations of

753 four cases of leak intensity noted in the figure as circled numbers.

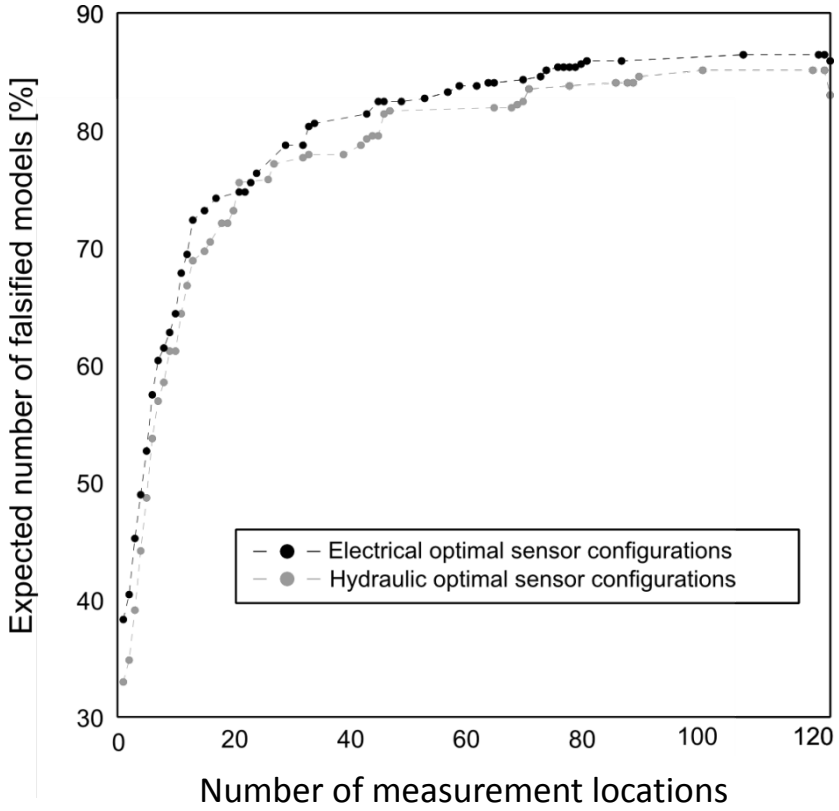

754

755

756 **Fig. 10.** Comparison of the curve that gives the relation between the expected number of
757 falsified leak scenarios (obtained through simulations with a probability of 95%) (Eq. 5) and
758 the number of measurements used.

759

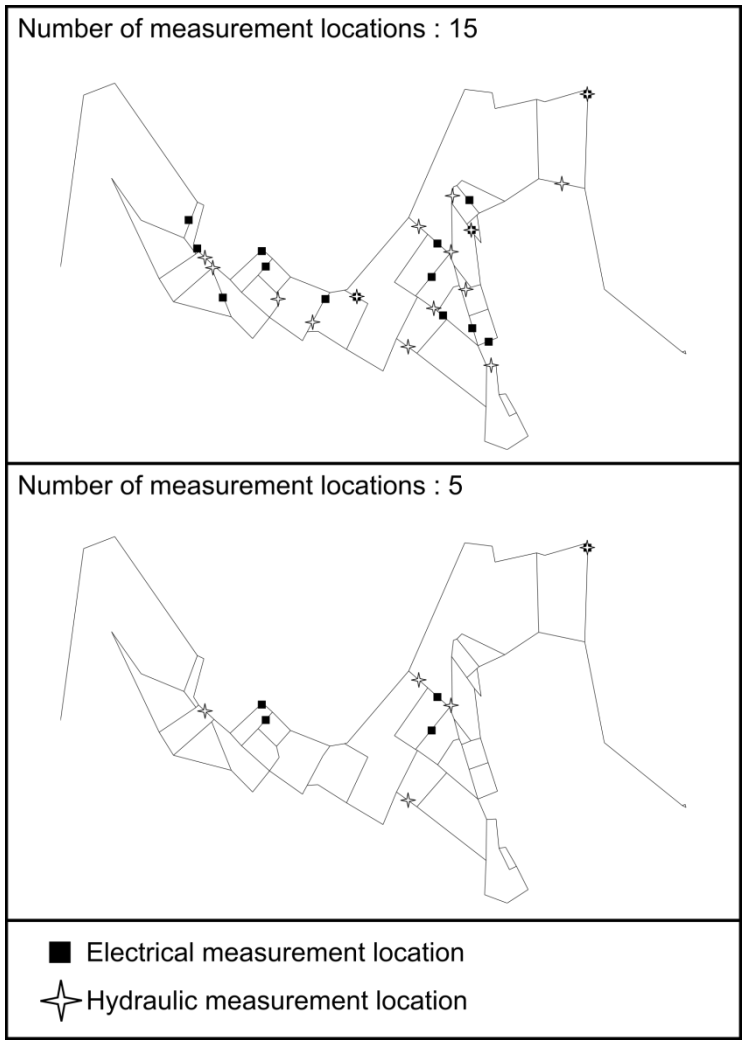

760

761

762 **Fig. 11.** Sensor placement results using simulation with a greedy algorithm for 15 and five

763 sensors.

764

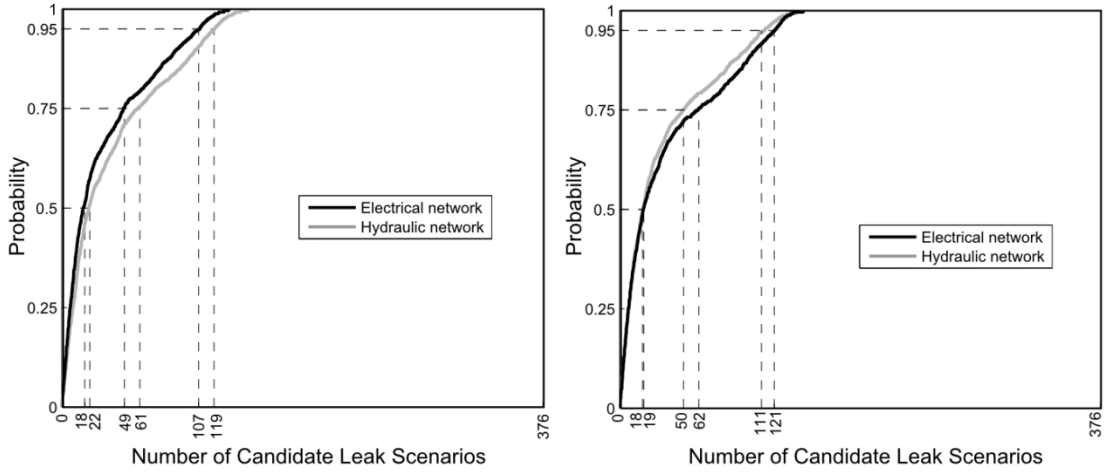

(a) (b)

Fig. 12. Comparison of expected identifiability (Fig. 6) using simulations of the electrical and hydraulic networks with the 15 sensor configuration obtained using the Greedy algorithm for a) the electrical model and b) the hydraulic model.

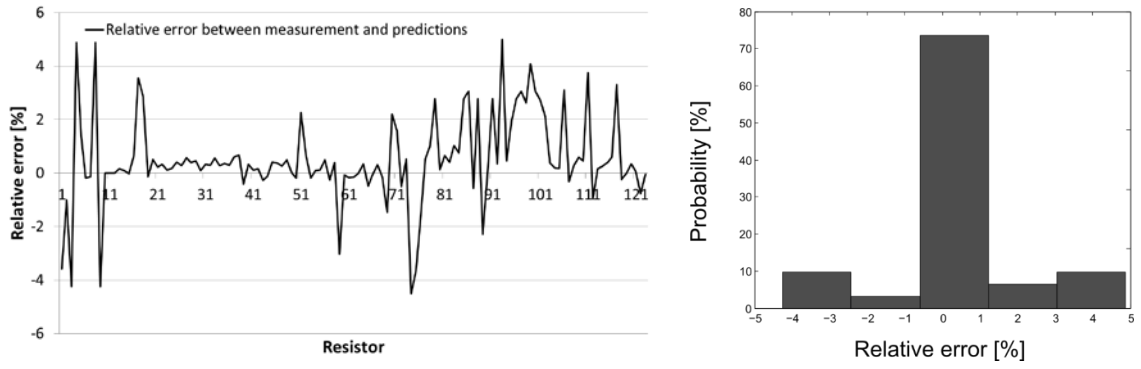

(a) (b)

Fig. 13. Relative error between measurements of the physical electrical network and predictions for each sensor.

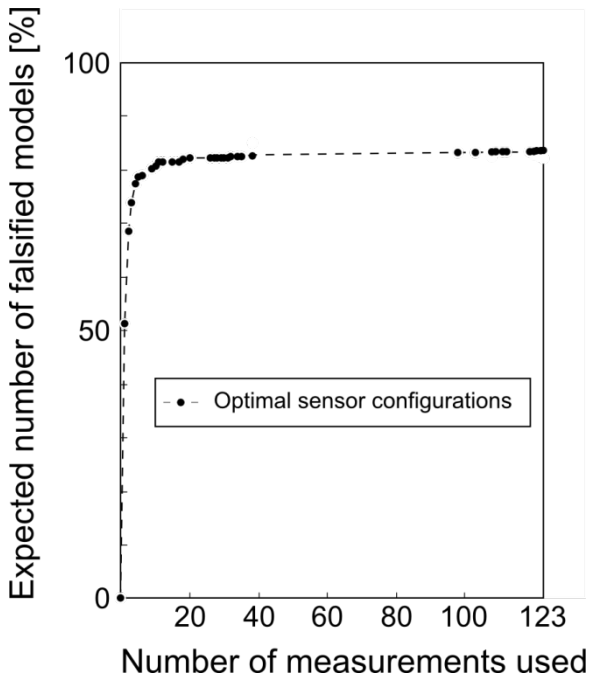

Fig. 14. The relation between the expected numbers of falsified leak scenarios (simulations with a probability of 95%) (Eq. 5) and the number of measurements.

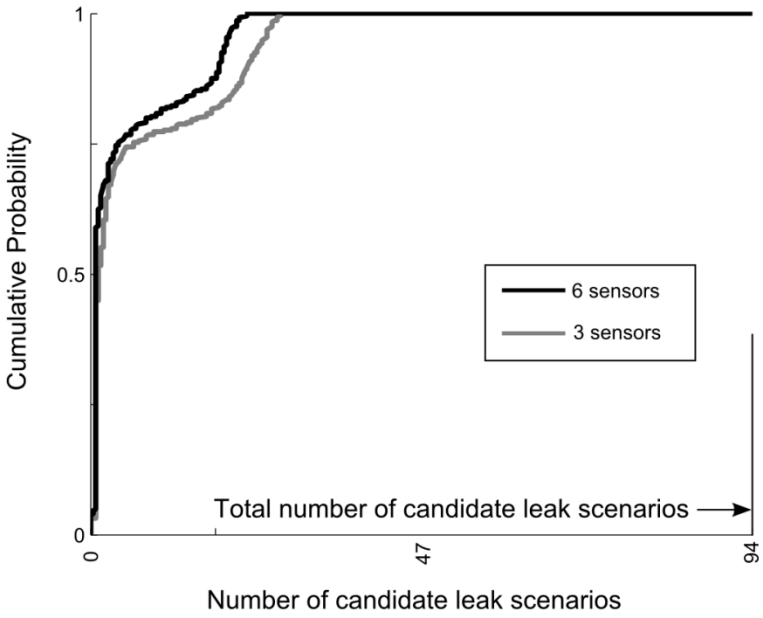

Fig. 15. Expected identifiability (Fig. 6) for simulations of three and six sensor configurations, for a current loss of 0.002 mA.

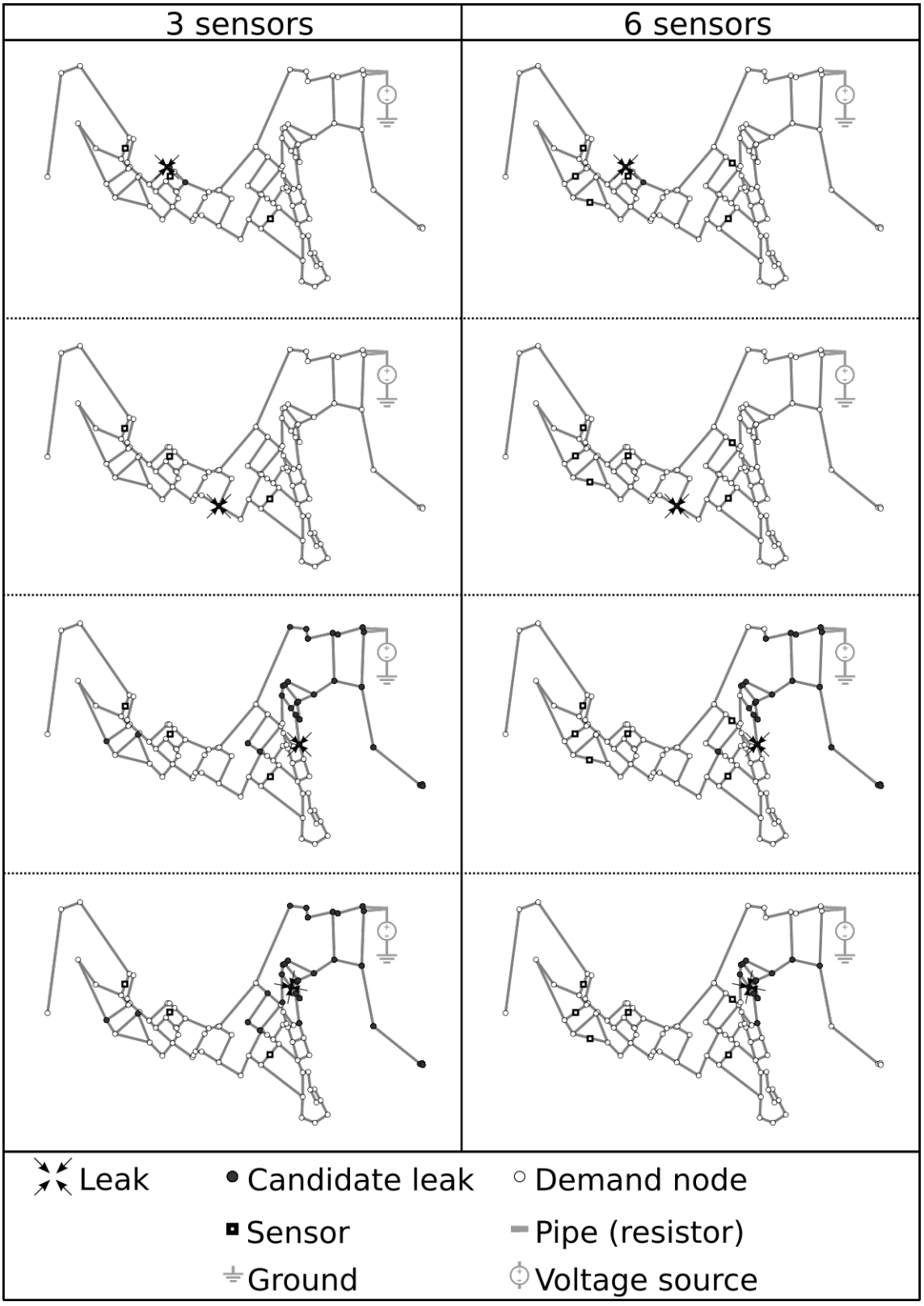

Fig. 16. Leak-region detection for laboratory measurements on physical electrical networks having four leak locations and two sensor configurations for a current loss of 0.002 mA.

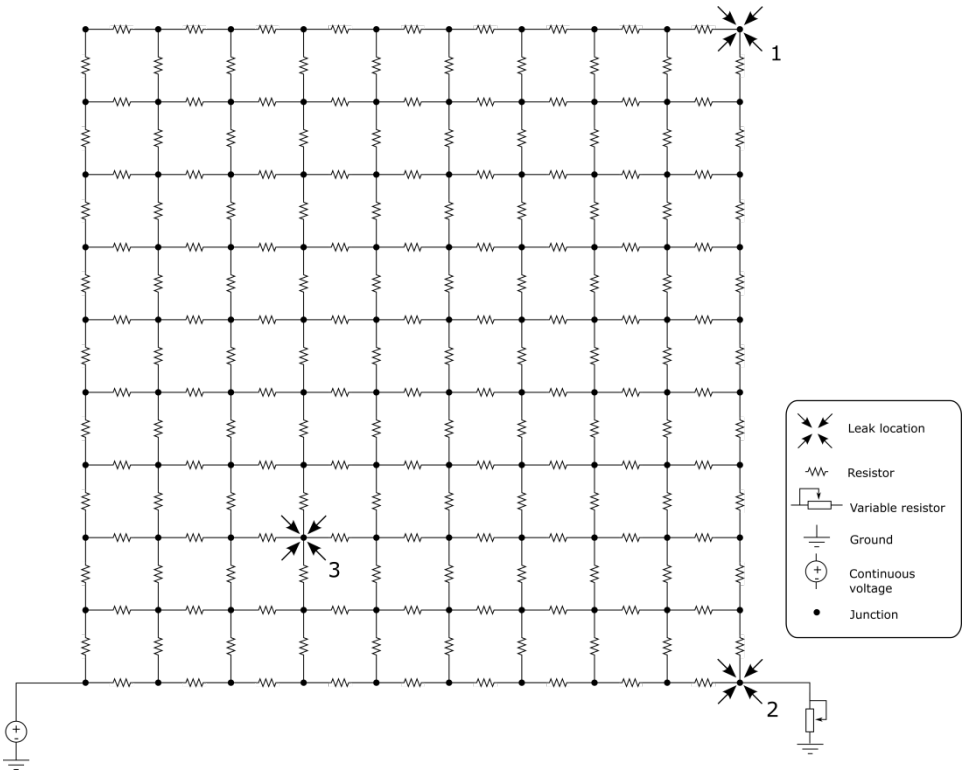

Fig. 17. Illustration of the 10x10 square electrical network.

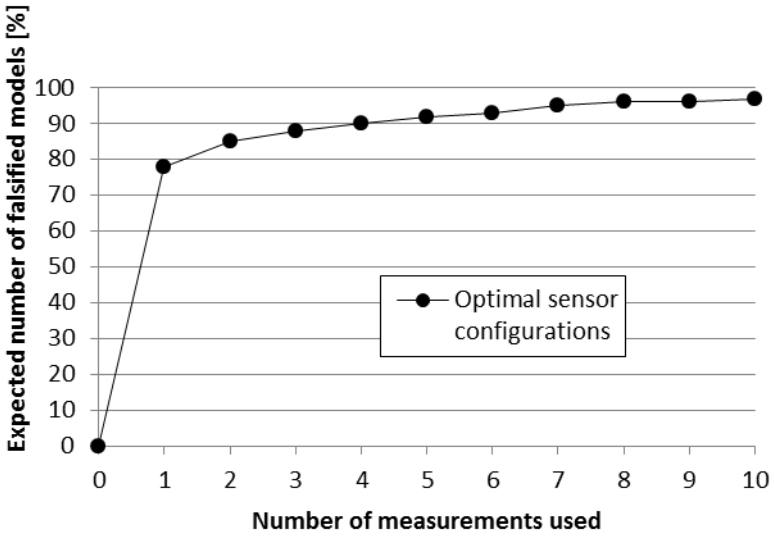

Fig. 18. The relation between the expected numbers of falsified models obtained through simulations (Eq. 5) and the number of measurements.

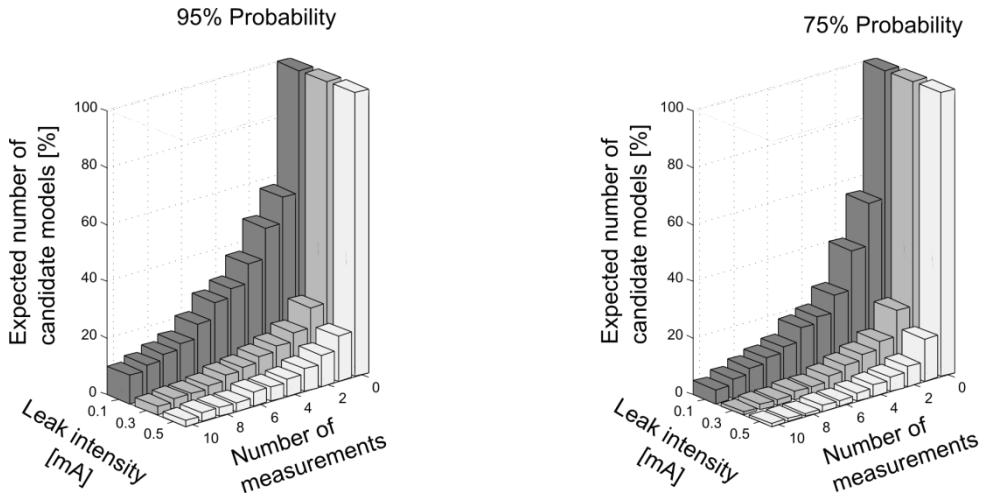

Fig. 19. Simulation results revealing the expected number of candidate models as a function of the leak intensity and the number of measurements for a 95% probability (left) and a 75% probability (right).

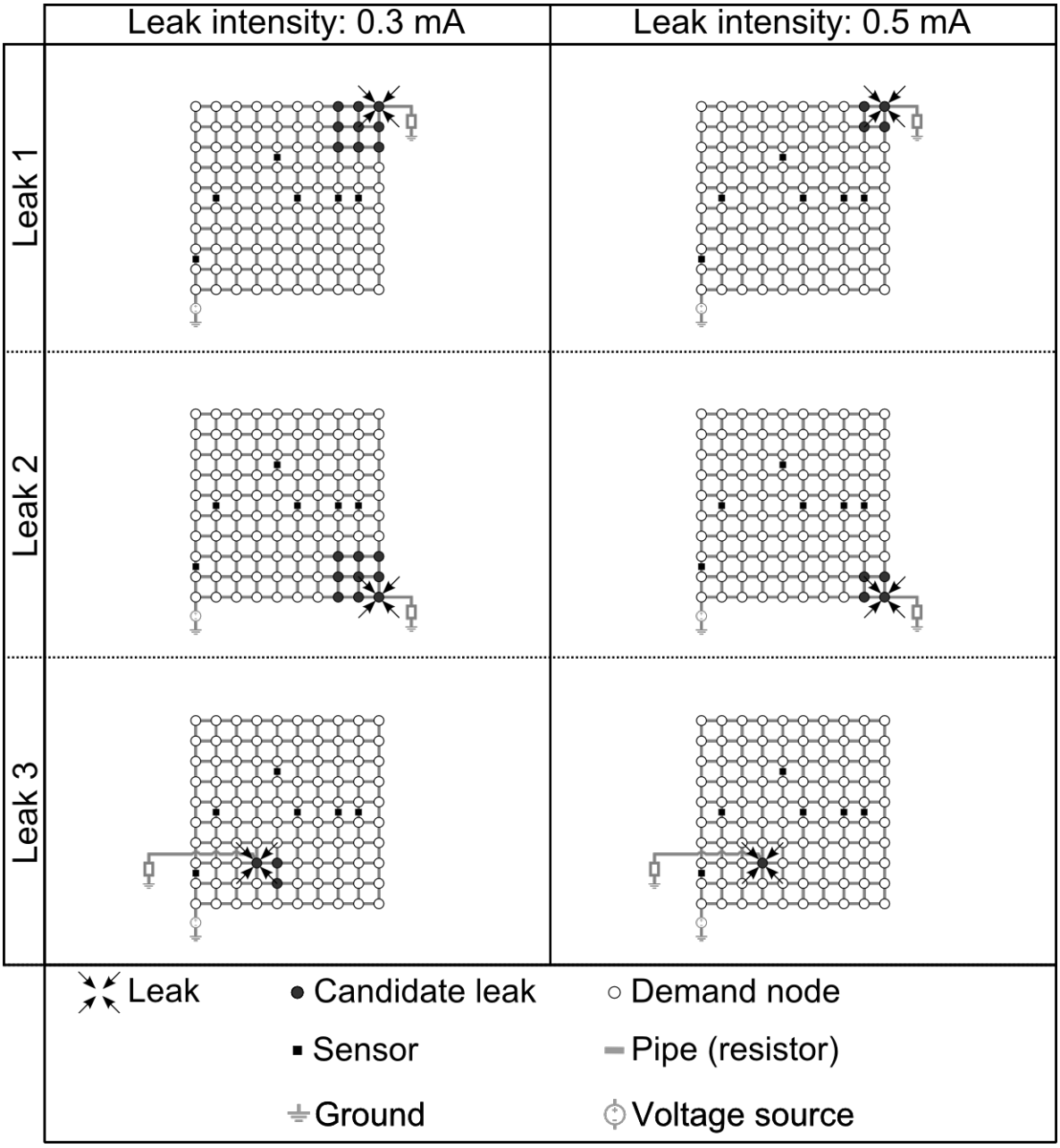

Fig. 20. Leak-region detection results for sensor measurements and leaks in the physical 10x10 electrical network.

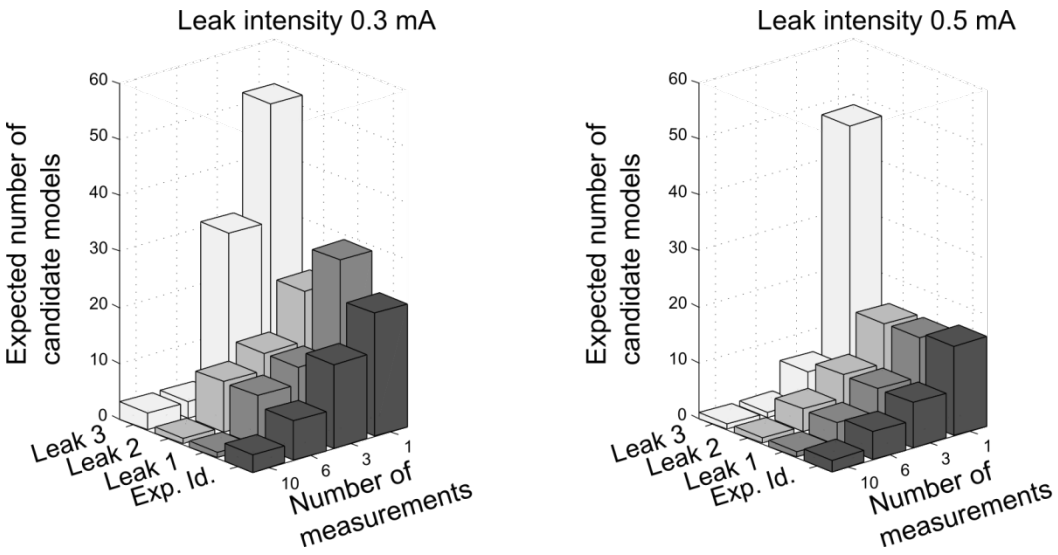

816

817

818 Fig. 21. Comparison between results obtained with real measurements on the physical
819 network (Leak 1-3) and expected identifiability (Exp. Id.) obtained through simulations (Fig.
820 6).

821

822

823 This work is licensed under a Creative Commons Attribution-NonCommercial-NoDerivatives
824 4.0 International License

825